Order-One Rolling Shutter Cameras

Marvin Anas Hahn
Trinity College Dublin
17 Westland Row, Dublin Ireland
hahnma@maths.tcd.ie

Kathlén Kohn
KTH Royal Institute of Technology
Lindstedtsvägen 25, 10044 Stockholm, Sweden
kathlen@kth.se

Orlando Marigliano
University of Genoa
Via Dodecaneso 35, 16146 Genoa, Italy
orlando.marigliano@edu.unige.it

Tomas Pajdla
CIIRC, Czech Technical University in Prague
Czech Republic
pajdla@cvut.cz

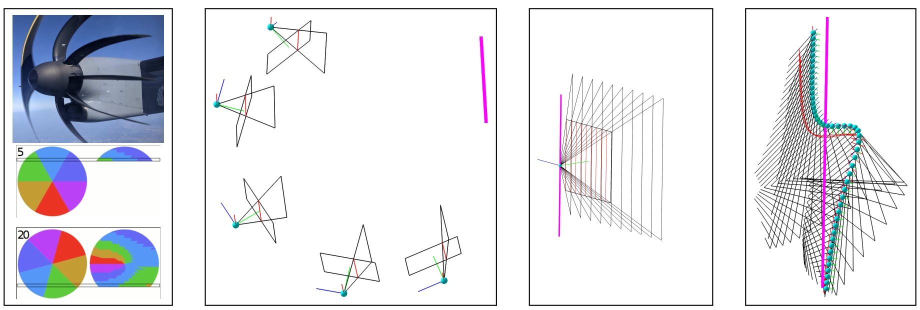

(a) (b) (c) (d)

Figure 1. (a) General rolling shutter cameras see points in space multiple times (en.wikipedia.org/wiki/Rolling_shutter). (b) Order-one rolling shutter cameras see points in space exactly once. Their rolling planes intersect in a line. Examples include (c) perspective cameras and (d) some Straight-Cayley cameras moving on a twisted cubic.

Abstract

Rolling shutter (RS) cameras dominate consumer and smartphone markets. Several methods for computing the absolute pose of RS cameras have appeared in the last 20 years, but the relative pose problem has not been fully solved yet. We provide a unified theory for the important class of order-one rolling shutter (RS_1) cameras. These cameras generalize the perspective projection to RS cameras, projecting a generic space point to exactly one image point via a rational map. We introduce a new back-projection RS camera model, characterize RS_1 cameras, construct explicit parameterizations of such cameras, and determine the image of a space line. We classify all minimal problems for solving the relative camera pose problem with linear RS_1 cameras and discover new practical cases. Finally, we show how the theory can be used to explain RS models previously used for absolute pose computation.

1. Introduction

Rolling shutter (RS) cameras [41] dominate consumer and smartphone markets thanks to affordability, enhanced resolution, and rapid frame rates. Unlike global shutter cameras (GS), RS cameras capture images sequentially line-by-line, causing image distortions if the camera moves during capture (Fig. 1a). The distorted RS images do not match the geometry of GS cameras. Thus, for non-negligible movements, the developed multi-view geometry for GS cameras cannot be applied. So currently, accurate multi-view geometry from moving cameras requires GS cameras. Since moving cameras are omnipresent (e.g., every modern car is equipped with cameras and cameras are often mounted on drones), new theory and algorithms must be developed for RS cameras. Many partial results appeared in the last 20 years [1, 2, 4–10, 12, 16–19, 24, 27, 29, 31, 33, 34, 37, 38, 40, 42, 43, 49–51, 54–58]. Here, we provide a unified theory and extend multi-view GS geometry to the important class of moving order-one RS cameras.

General RS cameras project a point in space into many

KK and OM were supported by Göran Gustafssons Stiftelse and Wallenberg AI, Autonomous Systems and Software Program (WASP) funded by Knut and Alice Wallenberg Foundation. OM was supported by the EU (Project 101061315–MIAS–HORIZON-MSCA-2021-PF-01) and TP by OPJAK CZ.02.01.01/00/22_008/0004590 Roboprox.

image points (Fig. 1a). Perspective cameras project a point in space by a linear rational map to exactly one image point. Thus, it is natural to study a generalization of perspective cameras: RS cameras that project a point in space to exactly one image point via a rational map. We call these *Order-one Rolling Shutter (RS_1)* cameras. RS_1 are relatively simple but can still explain some common scenarios. For instance, they can be used when RS images are taken on vehicles moving at constant speed on a straight line parallel to the image plane, which is common for cars, trains, planes, etc. Moreover, every flatbed scanner is an RS_1 camera, and satellite imaging is often done with push-broom scanners [23], which are very close to RS_1 cameras.

1.1. Contribution and main results

We present a systematic study of RS and RS_1 cameras.

In Sec. 2, we introduce a new back-projection model of RS cameras that provides explicit parameterizations of RS camera-rays via a map Λ (5) and of RS camera rolling planes via a map Σ (2). Our model connects the geometry of rays in space with the image projection maps of RS cameras. The map Λ assigns to every image point the ray in space that projects to the point. In general, this map has no inverse for RS cameras that see space points several times.

RS_1 cameras are precisely those where such an inverse picture-taking map $\Phi = \Lambda^{-1}$ exists and is rational. We analyze these maps in Sec. 3. We show (Theorem 4) that all rolling planes of an RS_1 camera intersect in a space line K. Furthermore, the rolling planes map Σ of such a camera is birational and the camera center moves on a curve $\mathcal{C}$ that either equals K or intersects K in $\deg(\mathcal{C}) - 1$ points.

In Sec. 4, we construct explicit parameterizations of RS_1 cameras. Explicit parameterizations open a way to identify camera parameters from image measurements. We give the dimensions of several RS_1 parameter spaces needed to characterize minimal problems (Sec. 6). We analyze the special cases of (1) constant rotation (Sec. 4.1) and (2) pure translation with a constant speed (Sec. 4.3), which were studied in [12] under the name *linear RS cameras*.

RS_1 cameras give rise to picture-taking maps Φ. In Sec. 5, we give the degree of Φ for all parameterizations of RS_1 cameras from Sec. 4 (see Theorem 12), and show that the image of a line in space is a rational image curve of degree $\deg(\Phi)$ that passes through a special point at infinity $\deg(\Phi) - 1$ many times. This means that the image of a space line contains precisely one further point at infinity. We use that point to simplify the camera relative pose minimal problems (see Sec. 6).

In Sec. 6, we present *all minimal problems* for computing the relative poses of linear RS_1 cameras from correspondences between multiple images of points and lines (with potential incidences) under complete visibility assumptions [25]. We show that there are exactly *31 minimal problems for 2, 3, 4, and 5 cameras* (Fig. 4). All these minimal problems are new. We also show that no minimal problems exist for a single camera and more than 5 cameras. For every minimal problem, we compute the number of solutions (degree). There are several practical minimal problems for two cameras: (i) Three problems with small degrees (28, 48, 60) and a small number of image features (e.g., 7 or 9 points, or 3 points + 2 lines) are suitable for constructing efficient symbolic-numeric minimal solvers [30, 35, 39]. (ii) Two important problems with 7 and 9 points have moderate degrees (140, 364) and thus are suitable for solving by optimized homotopy continuation [11, 15, 25]. Similarly, there is a practical problem for three cameras with degree 160. Minimal problems for more than three cameras are much harder and impractical unless they could be decomposed into simple problems [26]. This is an open problem for the future.

Sec. 7 shows when a practical "Straight-Cayley" (SC) RS camera model [7] produces RS_1 cameras. The SC model is important since it leads to tractable minimal RS camera absolute pose problems [7]. We provide explicit general constraints on the CS model and concrete examples. This demonstrates how the theory for RS_1 cameras developed in this paper can be used to understand existing practical RS camera models.

1.2. The most relevant previous work

[12] formulates the relative pose problems for two RS cameras for several RS models, but order-one cameras were not considered and camera order was not investigated. We show that general linear RS cameras have order two and that they have order one exactly when the motion line $\mathcal{C}$ is parallel to the camera projection plane. The uniform RS camera model of [12] uses the Rodrigues parameterization [22] of rotation, which is not algebraic. Hence, [12] replaces rotation matrices by their linearization to arrive at an approximate algebraic model. We use the Cayley rotation parameterization (20), which is algebraic, and we show when it produces RS_1 cameras. [12] observes that there is an 11-point minimal relative pose problem for two order-two linear RS cameras but does not present the solver. Instead, a rather impractical 20-point linear solver is suggested. We consider an RS_1 model and use all the algebraic constraints to get a solvable 9-point minimal relative RS_1 camera problem. We also classify all minimal problems for this model for arbitrarily many cameras (Fig. 4) and identify several practical RS camera relative pose problems.

[3, 7] developed efficient absolute pose minimal problems with the Straight-Cayley model. We show that the Straight-Cayley model is not only efficient but also very general and accounts for a large class of RS cameras, ranging from perspective cameras to many order-one cameras suitable for practical applications.

[47] studies linear congruences to model ray arrangements of generalized cameras [44, 46, 52]. It characterizes order-one congruences and together with its follow-up paper [53] introduces "photographic camera" projection maps that are rational. They study special two-slit cameras but do not relate the congruences and maps to RS cameras. We extend [47, 53] to real problems arising with RS cameras.

1.3. Concepts used in the main paper

We work with cameras that take pictures of points in projective 3-space $\mathbb{P}^3$ and produce points in the projective image plane $\mathbb{P}^2$. We often identify planes Σ in $\mathbb{P}^3$ with points $\Sigma^\vee$ in the dual space $(\mathbb{P}^3)^*$. The Grassmannian $\mathrm{Gr}(1,\mathbb{P}^3)$ is the set of lines in $\mathbb{P}^3$. For a line $L \in \mathrm{Gr}(1,\mathbb{P}^3)$, we write $L^\vee \subset (\mathbb{P}^3)^*$ for its dual line. The span of projective subspaces X and Y is denoted by $X \vee Y$. An *algebraic variety* is a solution set of polynomial equations. The *Zariski closure* of a set is the smallest algebraic variety containing the set. The *degree* of an algebraic curve $\mathcal{C}$ in $\mathbb{P}^3$ is the number of complex points in its intersection with a generic plane. We indicate rational functions, that are possibly not defined everywhere, via dashed arrows $\dashrightarrow$. A *birational map* is a rational function that is bijective onto its image almost everywhere (i.e., outside of a proper subvariety of the domain). Additional concepts, definitions, lemmas, and the proofs are included in SM.

2. Rolling shutter camera model

An *RS camera* is defined by moving a perspective camera with center C and projection plane Π in the space $\mathbb{P}^3$ while scanning the projection plane Π along a pencil $\mathcal{R}$ of (parallel) lines. The lines in this pencil are called *rolling image lines*. They capture the geometry of the rolling shutter effect. In applications, C, Π and lines $r \in \mathcal{R}$ are functions of time. However, typically, $\mathcal{R}$ is in one-to-one correspondence with a time interval. Thus, we use r to parameterize the camera motion and write $C(r)$ and $\Pi(r)$.

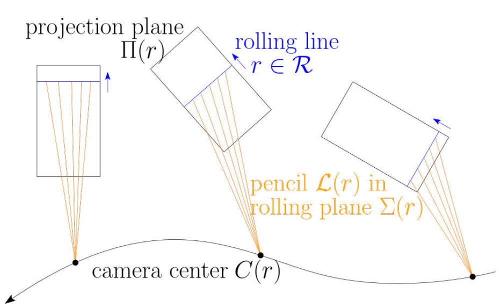

Figure 2. Overview of RS notation.

Each rolling line $r \in \mathcal{R}$ generates a rolling plane $\Sigma(r)$ that is the preimage of r for the perspective camera with center $C(r)$ and projection plane $\Pi(r)$. The points of $\Sigma(r) \subset \mathbb{P}^3$ are projected onto the rolling line $r \subset \mathbb{P}^2$ along the pencil $\mathcal{L}(r)$ of lines in $\Sigma(r)$ that pass through the center $C(r)$. The union $\mathcal{L} = \bigcup_{r\in\mathcal{R}} \mathcal{L}(r)$ of all pencils $\mathcal{L}(r)$ forms the set of rays of the RS camera; see Fig. 2.

To specify an RS camera model, we need to parameterize the pencil $\mathcal{R}$ of rolling lines in Π and couple it with a parameterization of the motion of the perspective camera in $\mathbb{P}^3$. We set the coordinate system in the plane $\mathbb{P}^2$ so that the rolling lines are parallel to the y-axis. The rolling-lines pencil $\mathcal{R}$ is then parameterized by the bijective morphism

$$\begin{aligned} &\rho : \mathbb{P}^1 \to \mathcal{R}, \\ &(v:t) \mapsto (0:1:0) \vee (v:0:t) \equiv (-t:0:v) \in (\mathbb{P}^2)^*. \end{aligned} \tag{1}$$

Considering the calibrated scenario [21], the camera position and orientation are defined on the affine chart $\mathbb{R}^1$ where $t \neq 0$. They are described by $C(\frac{v}{t}) \in \mathbb{R}^3$ and $R(\frac{v}{t}) \in \mathrm{SO}(3)$. This gives the corresponding projection matrix $P(\frac{v}{t}) := R(\frac{v}{t})\,[I_3 \mid -C(\frac{v}{t})] \in \mathbb{R}^{3\times 4}$ that represents a linear map $\mathbb{P}^3 \dashrightarrow \mathbb{P}^2$. Now, we can take the preimages of the rolling lines in $\mathcal{R}$ and obtain rolling planes in $\mathbb{P}^3$:

$$\Sigma^\vee : \mathbb{R}^1 \to (\mathbb{P}^3)^*, \tfrac{v}{t} \mapsto \Sigma(\tfrac{v}{t})^\vee = (1:0:-\tfrac{v}{t})\cdot P(\tfrac{v}{t}). \tag{2}$$

Now the set $\mathcal{L}$ of camera rays is determined: it is the union of the pencils $\mathcal{L}(\frac{v}{t}) := \{L \in \mathrm{Gr}(1,\mathbb{P}^3) \mid C(\frac{v}{t}) \in L \subset \Sigma(\frac{v}{t})\}$. A natural global parametrization of this union of pencils is given by taking preimages of image points on $r = \rho(\frac{v}{t}:1)$ under the projection matrix $P(\frac{v}{t})$. To parameterize the points on r, we intersect r with another conveniently chosen set of lines, reflecting pixels on images. For that, we make the standard choice, using lines parallel to the x-axis:

$$\begin{aligned} &\nu : \mathbb{P}^1 \to (\mathbb{P}^2)^*, \\ &(u:s) \mapsto (1:0:0) \vee (0:u:s) \equiv (0:-s:u) \in (\mathbb{P}^2)^*. \end{aligned} \tag{3}$$

An image point on the rolling line $r = \rho(v:t)$ is obtained by intersecting r with the line $\nu(u:s)$, which is captured by the birational map

$$\varphi : \mathbb{P}^1 \times \mathbb{P}^1 \dashrightarrow \mathbb{P}^2, ((v:t),(u:s)) \mapsto (sv:ut:st). \tag{4}$$

This map is not defined at the point $((1:0),(1:0))$, where both lines $\rho(1:0)$ and $\nu(1:0)$ equal the line at infinity. We obtain all camera rays in $\mathcal{L}$ by taking the preimages in $\mathbb{P}^3$ of the image points with affine coordinates $(\frac{u}{s},\frac{v}{t})$ under the projection matrix $P(\frac{v}{t})$ (see Sec. 9.1 for a derivation):

$$\begin{aligned} &\Lambda : \mathbb{R}^1 \times \mathbb{R}^1 \to \mathrm{Gr}(1,\mathbb{P}^3), \\ &(\tfrac{v}{t},\tfrac{u}{s}) \mapsto \begin{bmatrix} I_3 \\ -C(\frac{v}{t})^\top \end{bmatrix} \left[R(\tfrac{v}{t})^\top \begin{bmatrix} \frac{v}{t} \\ \frac{u}{s} \\ 1 \end{bmatrix} \right]_\times [I_3 \mid -C(\tfrac{v}{t})]. \end{aligned} \tag{5}$$

Here, given a vector $V \in \mathbb{R}^3$, we write $[V]_\times$ for the skew-symmetric 3×3 matrix that represents the linear map that takes the cross product with V. Then, $\Lambda(\frac{v}{t},\frac{u}{s})$ is a skew-symmetric 4×4 matrix whose entries are the dual Plücker coordinates of the camera ray that the camera maps to the image point $(\frac{v}{t}, \frac{u}{s})$, i.e., the (i,j)-th entry of $\Lambda(\frac{v}{t}, \frac{u}{s})$ is the determinant of the submatrix with columns (i,j) of the 2×4 matrix whose two rows are $(0:1:-\frac{u}{s})\cdot P(\frac{v}{t})$ and $\Sigma(\frac{v}{t})^\vee$.

The set $\mathcal{L}$ of all camera rays captures most of the essential geometry of the camera, while its parametrization Λ describes the concrete imaging process onto an actual picture plane [48]. Note that we used the term 'camera rays' for lines through the camera center, and not for actual rays in the sense of half-lines. This a good model for RS cameras with a view of less than 180 degrees. For more general modeling, we'd have to consider half-lines with orientation.

Remark 1. $G := \{[\begin{smallmatrix} R & t \\ 0 & \alpha \end{smallmatrix}] \mid R \in \mathrm{SO}(3), t \in \mathbb{R}^3, \alpha \in \mathbb{R} \setminus \{0\}\}$ is the scaled special Euclidean group on $\mathbb{R}^3$. It acts on the space of RS cameras. For a camera given by the projection-matrix map $P : \mathbb{R}^1 \to \mathbb{R}^{3\times 4}, \frac{v}{t} \mapsto P(\frac{v}{t})$ and a group element $g \in G$, the action is defined via

$$g.P := \left(\mathbb{R}^1 \to \mathbb{R}^{3\times 4},\ \tfrac{v}{t} \mapsto P(\tfrac{v}{t}) \cdot g\right). \tag{6}$$

When acting simultaneously on cameras and the world points $X \in \mathbb{P}^3$ via $g.X := g^{-1} \cdot X$, the imaging process stays invariant. Indeed, writing $g.\Lambda$ for the map (5) associated with the transformed projection $g.P = g.(R[I_3|-C])$, we have that the line $(g.\Lambda)(\frac{v}{t}, \frac{u}{s})$ is the image of the line $\Lambda(\frac{v}{t}, \frac{u}{s})$ under the G-action on $\mathbb{P}^3$. This means that 3D reconstruction using our camera model is only possible up to a proper rigid motion and a non-zero scale, when we do not fix any RS camera's scale (e.g., by knowing ray distances).

3. Order-one cameras

In this article, we analyze RS cameras that see a generic (i.e., sufficiently random) point in 3-space exactly once, i.e., a generic space point appears exactly once on the image plane $\mathbb{P}^2$. For that to happen, two conditions need to be satisfied: 1) For a generic point in $\mathbb{P}^3$, there has to be a unique camera ray in $\mathcal{L}$ passing through it. 2) The camera ray has to correspond to a unique point on the image plane via the map Λ. We classify all RS cameras satisfying those conditions, where we additionally impose the imaging process to be algebraic, i.e., we require Λ to be a rational map.

The rationality of the map Λ implies that both the rolling planes map Σ and the center-movement map $C : \mathbb{R}^1 \to \mathbb{R}^3$ are rational (Lemma 24). In that case, the *center locus* $\mathcal{C}$, i.e., the Zariski closure in $\mathbb{P}^3$ of the image of C, is either a point or a rational curve. Moreover, the Zariski closure $\overline{\mathcal{L}}$ of the set $\mathcal{L}$ of camera rays inside the Grassmannian $\mathrm{Gr}(1,\mathbb{P}^3)$ is a surface (or a one-dimensional pencil in the degenerate case when the center locus $\mathcal{C}$ is a single point and all rolling planes are equal); see Lemma 25. Such a surface in $\mathrm{Gr}(1,\mathbb{P}^3)$ is classically called a *line congruence* [28]. An important invariance of such a congruence is its order. The *order* is the number of lines on the congruence that pass through a generic space point. Hence, we are interested in RS cameras whose associated congruence $\overline{\mathcal{L}}$ has order one.

Definition 2. We say that a RS camera has *order one* if its associated congruence $\overline{\mathcal{L}}$ has order one and its parametrization Λ is birational; in other words, if it projects a generic point in space to exactly one image point via a rational map. We shortly write *RS_1 camera* for a RS camera of order one.

For RS_1 cameras, the image projection is a rational function $\Phi : \mathbb{P}^3 \dashrightarrow \mathbb{P}^2$, which we can explicitly describe as follows: The congruence $\overline{\mathcal{L}}$ has order one if and only if there is a map $\Gamma : \mathbb{P}^3 \dashrightarrow \overline{\mathcal{L}}$ from (a Zariski dense subset of) $\mathbb{P}^3$ to the camera rays that assigns to a visible point X the unique ray that sees it. The map Λ is birational if and only if it is rational and (almost everywhere) invertible, which means that the camera ray $\Gamma(X)$ corresponds to the unique image point $\Lambda^{-1}(\Gamma(X))$. The inverse map Λ^{-1} is rational as well. Thus, using the embedding $\mathbb{R}^1 \times \mathbb{R}^1 \subset \mathbb{P}^1 \times \mathbb{P}^1$, taking a picture of a generic space point $X \in \mathbb{P}^3$ is the rational map

$$\Phi : \mathbb{P}^3 \dashrightarrow \mathbb{P}^2, \quad X \longmapsto \varphi(\Lambda^{-1}(\Gamma(X))). \tag{7}$$

Example 3. A familiar RS_1 camera is the static pinhole camera. Its congruence $\overline{\mathcal{L}}$ consists of all lines passing through the fixed camera center C. The map Γ assigns to each space point $X \neq C$ the camera ray spanned by C and X. That ray intersects the static projection plane $\Pi \cong \mathbb{P}^2$ in the unique point $\Phi(X)$.

Theorem 4. *Consider a RS camera whose congruence-parametrization map Λ is rational. The camera has order one if and only if the intersection of all rolling planes $\Sigma(\frac{v}{t})$ is a line K, the rolling planes map Σ is birational, and its center locus $\mathcal{C}$ is one of the following:*
I. $\mathcal{C}$ is a rational curve & meets K in $\deg \mathcal{C} - 1$ many points,
II. or $\mathcal{C} = K$,
III. or $\mathcal{C}$ is a point on K.

Remark 5. In type I, the points in the intersection $\mathcal{C} \cap K$ are counted with multiplicity. Also, the maps Σ and C determine each other: Whenever $C(\frac{v}{t}) \notin K$, we have $\Sigma(\frac{v}{t}) = K \vee C(\frac{v}{t})$. Conversely, every rolling plane $\Sigma(\frac{v}{t})$ meets $\mathcal{C}$ in $\deg \mathcal{C}$ many points (counted with multiplicity), out of which all but one lie on the line K. The remaining point is $C(\frac{v}{t})$. In particular, since Σ is birational, so is C.

4. Building RS_1 cameras

Theorem 4 is constructive, meaning that we can use it to build – in theory – all RS_1 cameras. In the following, we describe the spaces of all RS_1 cameras of types I, II, and III (see Sec. 10). We start with type I. For that, we consider

$$\mathcal{H}_d := \{(\mathcal{C}, K) \mid \mathcal{C} \subset \mathbb{P}^3 \text{ rational curve of degree } d, \\ K \subset \mathbb{P}^3 \text{ line},\ \#(K \cap \mathcal{C}) = d-1\}, \tag{8}$$

where $\#$ counts with multiplicities. We can explicitly pick elements in this parameter space as follows: Choose a line K. Rotate and translate until K becomes the z-axis $K' := (0:0:1:0) \vee (0:0:0:1)$. Every curve $\mathcal{C}'$ with $(\mathcal{C}', K') \in \mathcal{H}_d$ is parametrized by $\mathbb{P}^1 \dashrightarrow \mathbb{P}^3, (v:t) \mapsto (vf(v:t) : tf(v:t) : g(v:t) : h(v:t))$, where f, g, h are homogeneous polynomials of degree $d-1, d, d$ [48, Eqn. (18)]. Reverse the translation and rotation to obtain $(\mathcal{C}, K) \in \mathcal{H}_d$.

Picking elements in $\mathcal{H}_d$ allows us to parametrize all RS_1 cameras of type I. For that, let H^∞ be the plane at infinity $(0:0:0:1)^\vee \subseteq \mathbb{P}^3$. We denote the intersection of a variety $\mathcal{V} \subseteq \mathbb{P}^3$ with H^∞ by $\mathcal{V}^\infty$. For a map $\Sigma^\vee : \mathbb{P}^1 \dashrightarrow (\mathbb{P}^3)^*$, we define $\Sigma^\vee_\infty(v:t) \in (H^\infty)^*$ as the projection of $\Sigma^\vee(v:t)$ to $(H^\infty)^*$. In the primal $\mathbb{P}^3$, this is the line in the intersection of the planes $\Sigma(v:t)$ and H^∞. For vectors A, B, we write $A \cdot B$ for the bilinear form $\sum_i A_i B_i$.

Proposition 6. *The RS_1 cameras of type I are in 4-to-1 correspondence with the parameter space*

$$\begin{aligned} \mathcal{P}_{I,d,\delta} := \{ &(K, \mathcal{C}, \Sigma^\vee_\infty, \lambda) \mid (\mathcal{C}, K) \in \mathcal{H}_d, \\ &\mathcal{C}^\infty \neq \mathcal{C},\, K^\infty \neq K,\, \lambda : \mathbb{P}^1 \dashrightarrow K,\, \deg(\lambda) = \delta, \\ &\Sigma^\vee_\infty : \mathbb{P}^1 \dashrightarrow (K^\infty)^\vee, (v:t) \mapsto Av + Bt \text{ for some} \\ &A, B \text{ with } A \cdot B = 0 \text{ and } A \cdot A = B \cdot B \}. \end{aligned} \tag{9}$$

The dimension of this space is $\dim \mathcal{P}_{I,d,\delta} = 3d + 2\delta + 7$.

Each element $(K, \mathcal{C}, \Sigma^\vee_\infty, \lambda)$ in $\mathcal{P}_{I,d,\delta}$ corresponds to four RS_1 cameras as follows (see Fig. 3): The rolling planes map Σ of the cameras can be read off from the the map $\Sigma^\vee_\infty$ since each rolling plane $\Sigma(v:t)$ is the span of the line $\Sigma_\infty(v:t)$ with K. By Remark 5, the map Σ determines uniquely the parametrization C of the curve $\mathcal{C}$, i.e., the movement of the camera center. The camera rotation map $R : \mathbb{R} \to \mathrm{SO}(3)$ is fixed as follows: For $x \in \mathbb{R}$, $R(x)$ has three degrees of freedom. The first two are accounted for by the rolling plane $\Sigma(x)$. Here, we have to choose an orientation / sign of the normal vector of the plane $\Sigma(x)$, since this is not encoded in the projective map Σ. Finally, the map $\lambda : \mathbb{P}^1 \dashrightarrow K$ chooses the unique point $\lambda(x)$ on K that the projection matrix $P(x)$ maps to $(0:1:0)$, the intersection point of all rolling lines. Thus, $\lambda(x)$ fixes the third degree of freedom of $R(x)$, but its sign gives us again two choices. In summary, the two choices of orientation, that on Σ and that on λ, give us 4 rotation maps $R : \mathbb{R} \to \mathrm{SO}(3)$.

Remark 7. For every line, conic, or non-planar rational curve $\mathcal{C}$ of degree at most five, there is a RS_1 camera moving along $\mathcal{C}$. For a generic rational curve of degree at least six, there is no such camera.

Proposition 8. *The RS_1 cameras of type II are in 4-to-1 correspondence with*

$$\begin{aligned} \mathcal{P}_{II,d,\delta} := \{ &(K, C, \Sigma^\vee_\infty, h, p) \mid K \in \mathrm{Gr}(1, \mathbb{P}^3), \\ &K^\infty \neq K,\, C : \mathbb{P}^1 \dashrightarrow K,\, \deg(C) = d, \\ &\Sigma^\vee_\infty : \mathbb{P}^1 \dashrightarrow (K^\infty)^\vee, (v:t) \mapsto Av + Bt \text{ for some} \\ &A, B \text{ with } A \cdot B = 0 \;\&\; A \cdot A = B \cdot B, \\ &(h, p) \in \mathbb{P}(\mathbb{R}[v,t]_\delta \times \mathbb{R}[v,t]_{\delta+d+1}) \}. \end{aligned} \tag{10}$$

RS_1 cameras of type III are the special case when $d = 0$ and the image of the constant map C is not at infinity. Moreover, $\dim \mathcal{P}_{II,d,\delta} = 3d + 2\delta + 8$.

An element $(K, C, \Sigma^\vee_\infty, h, p)$ in $\mathcal{P}_{II,d,\delta}$ gives rise to 4 RS_1 cameras as follows: C describes the movement of the camera center. As above, the map $\Sigma^\vee_\infty$ determines the rolling planes map Σ, which fixes (up to orientation) 2 degrees of freedom of each rotation $R(x)$ for $x \in \mathbb{R}$. To fix the 3rd degree, we assume (by rotating and translating) that K is the z-axis. Then, $C = (0:0:C_3:C_0)$, where C_3, C_0 are homogeneous of degree d, and $\Sigma^\vee = (\Sigma_1 : \Sigma_2 : 0 : 0)$ with Σ_1, Σ_2 homogeneous linear. The polynomials h, p define a map $\xi : \mathbb{P}^1 \dashrightarrow \mathrm{Gr}(1, \mathbb{P}^3)$ in Plücker coordinates: $(0 : -h\Sigma_2 C_3 : -h\Sigma_2 C_0 : h\Sigma_1 C_3 : h\Sigma_1 C_0 : p)$[1]. This map satisfies $C(v:t) \in \xi(v:t) \subseteq \Sigma(v:t)$ for all $(v:t) \in \mathbb{P}^1$ (see Lemma 38). It chooses the unique camera ray $\xi(x)$ that the projection matrix $P(x)$ maps to $(0:1:0)$. So, up to sign, $\xi(x)$ fixes $R(x)$. The two choices of orientation, that on Σ and that on ξ, give us 4 rotation maps $R : \mathbb{R} \to \mathrm{SO}(3)$.

4.1. Constant rotation

In the special case that cameras do not rotate, we can more easily check whether the order is 1. In fact, the center-movement map C is rational iff Λ is rational (see (5) and Lemma 24), and the condition that all rolling planes meet in a line implies all other conditions in Theorem 4.

Proposition 9. *A RS camera with constant rotation and rational center movement has order one if and only if the intersection of all its rolling planes is a line.*

We denote the three rows of the constant rotation matrix $R \in \mathrm{SO}(3)$ by w_1, w_2, w_3. Then, we can write the rolling planes map (2) as $\Sigma : (v:t) \mapsto (w_2 : 0) \vee (vw_1 + tw_3 : 0) \vee C(v:t)$. In particular, all rolling planes go through the point $(w_2 : 0)$. When the intersection of the rolling planes is a line K, then $(w_2 : 0)$ is the unique point of intersection of K with the plane at infinity. (Otherwise, if K were contained in that plane, then all rolling planes would be equal to that plane.) In particular, the line K determines the second row of R (up to sign) and the remaining rows of R determine the rolling planes map as

$$\Sigma : (v:t) \mapsto K \vee (vw_1 + tw_3 : 0). \tag{11}$$

So, for constant rotation, the spaces of RS_1 cameras are

$$\begin{aligned} \mathcal{P}_{I,d} := \{ &(R, K, \mathcal{C}) \mid R \in \mathrm{SO}(3) \text{ with 2nd row } w_2, \\ &K \in \mathrm{Gr}(1, \mathbb{P}^3),\, K^\infty = (w_2 : 0), (\mathcal{C}, K) \in \mathcal{H}_d \}, \end{aligned} \tag{12}$$

$$\begin{aligned} \mathcal{P}_{II,d} := \{ &(R, K, C) \mid R \in \mathrm{SO}(3) \text{ with 2nd row } w_2, \\ &K \in \mathrm{Gr}(1, \mathbb{P}^3),\, K^\infty = (w_2 : 0), C : \mathbb{P}^1 \dashrightarrow K,\, \deg(C) = d \} \end{aligned} \tag{13}$$

and $\mathcal{P}_{II,0}$ (with $\mathrm{im}(C) \neq K^\infty$) is the space of static pinhole cameras; note $\dim \mathcal{P}_{I,d} = 3d + 6$ and $\dim \mathcal{P}_{II,d} = 2d + 6$.

[1] The Plücker coordinates $(p_{12} : p_{13} : p_{10} : p_{23} : p_{20} : p_{30})$ of the line spanned by $(a_1 : a_2 : a_3 : a_0)$ and $(b_1 : b_2 : b_3 : b_0)$ are $p_{ij} = a_i b_j - a_j b_i$.

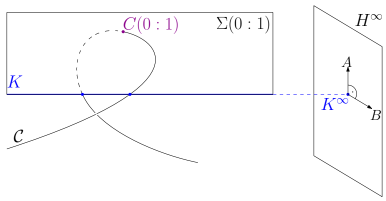

Figure 3. Illustration of $\mathcal{P}_{1,3,\delta}$: E.g., the rolling plane $\Sigma(0:1)$ meets the infinity plane H^∞ at a line with normal vector B.

4.2. Moving along a line with constant speed

In many applications, where the camera moves along a line, it moves with approximately constant speed. Projectively, this means that the parameterization C of the line $\mathcal{C}$ is birational with $C(1:0)=\mathcal{C}^\infty$. In the case of RS_1 cameras of type I, this means that $\Sigma(1:0)=K\vee\mathcal{C}^\infty$ is already determined by K and $\mathcal{C}$, and cannot be freely chosen. Thus, the space of such RS_1 cameras is

$$\begin{aligned}\mathcal{P}^{\mathrm{cs}}_{I,1,\delta} := \{&(K,\mathcal{C},\Sigma^\vee_\infty,\lambda) \mid K,\mathcal{C}\in \mathrm{Gr}(1,\mathbb{P}^3),\\ &\mathcal{C}^\infty\neq\mathcal{C},\ K^\infty\neq K,\ K\cap\mathcal{C}=\emptyset,\\ &\Sigma^\vee_\infty:\mathbb{P}^1 \dashrightarrow (K^\infty)^\vee, (v:t)\mapsto Av+Bt, \text{ where}\\ &A=(K^\infty\vee\mathcal{C}^\infty)^\vee,\ A\cdot B=0, A\cdot A=B\cdot B,\\ &\lambda:\mathbb{P}^1\dashrightarrow K,\ \deg(\lambda)=\delta\}\end{aligned} \tag{14}$$

The dimension of this space is one less than the space $\mathcal{P}_{I,1,\delta}$ without the constant-speed assumption, i.e., $\dim\mathcal{P}^{\mathrm{cs}}_{I,1,\delta}=2\delta+9$, as the birational map $\Sigma^\vee_\infty$ is already prescribed. In fact, over $\mathbb{R}$, there are two such maps since the coefficient vector B can be scaled by -1. Similarly, the space of constant-speed RS_1 cameras of type II is

$$\begin{aligned}\mathcal{P}^{\mathrm{cs}}_{II,1,\delta}:=\{&(K,C,\Sigma^\vee_\infty,h,p) \mid K\in\mathrm{Gr}(1,\mathbb{P}^3), K^\infty\neq K,\\ &C:\mathbb{P}^1\dashrightarrow K \text{ birational}, C(1:0)=K^\infty,\\ &\Sigma^\infty:\mathbb{P}^1\dashrightarrow(K^\infty)^\vee, (v:t)\mapsto Av+Bt \text{ for some}\\ &A,B \text{ with } A\cdot B=0, A\cdot A=B\cdot B,\\ &(h,p)\in\mathbb{P}(\mathbb{R}[v,t]_\delta\times\mathbb{R}[v,t]_{\delta+2})\}\end{aligned} \tag{15}$$

and has dimension $\dim\mathcal{P}^{\mathrm{cs}}_{II,1,\delta}=2\delta+10$.

4.3. Linear RS_1 cameras

As in [12], we call a RS camera that does not rotate and moves along a line with constant speed a *linear RS camera*. We describe such cameras of order one. Since, in type I, constant speed means $\Sigma(1:0)=K\vee\mathcal{C}^\infty$, (11) implies that the point $\mathcal{C}^\infty$ has to lie on the line in the infinity plane that is spanned by the first two 2 of the fixed rotation matrix R:

$$\begin{aligned}\mathcal{P}^{\mathrm{cs}}_{I,1}:=\{&(R,K,\mathcal{C}) \mid R=\left[\begin{smallmatrix}w_1\\w_2\\w_3\end{smallmatrix}\right]\in\mathrm{SO}(3),\\ &K\in\mathrm{Gr}(1,\mathbb{P}^3),\ K^\infty=(w_2:0),\ \mathcal{C}\in\mathrm{Gr}(1,\mathbb{P}^3),\\ &K\cap\mathcal{C}=\emptyset,\ \mathcal{C}^\infty\in(w_1:0)\vee(w_2:0)\}.\end{aligned} \tag{16}$$

Since the rotation is constant, the embedded projection plane $\Pi(v:t)$ of the camera is only affected by parallel translation. It stays always parallel to the plane spanned by w_1, w_2 and the origin in $\mathbb{R}^3$. Projectively, this means that $\Pi(v:t)^\infty=(w_1:0)\vee(w_2:0)$ for all $(v:t)\in\mathbb{P}^1$. Hence, the last condition in the definition of $\mathcal{P}^{\mathrm{cs}}_{I,1}$ means that the line $\mathcal{C}$ has to be parallel to the projection plane Π. In particular, the projection plane does not change at all over time.

For linear RS_1 cameras of type II, we have analogously

$$\begin{aligned}\mathcal{P}^{\mathrm{cs}}_{II,1}:=\{&(R,K,C) \mid R\in\mathrm{SO}(3) \text{ with 2nd row } w_2,\\ &K\in\mathrm{Gr}(1,\mathbb{P}^3),\ K^\infty=(w_2:0),\\ &C:\mathbb{P}^1\dashrightarrow K \text{ birational},\ C(1:0)=K^\infty\}.\end{aligned} \tag{17}$$

The dimensions of these spaces are $\dim\mathcal{P}^{\mathrm{cs}}_{I,1}=3+2+3=8$ and $\dim\mathcal{P}^{\mathrm{cs}}_{II,1}=3+2+2=7$. By the following proposition, we can put $\mathcal{P}^{\mathrm{cs}}_{I,1}$ and $\mathcal{P}^{\mathrm{cs}}_{II,1}$ into a joint parameter space.

Proposition 10. *A linear RS camera (i.e., that moves with constant speed along a line $\mathcal{C}\subseteq\mathbb{P}^3$ and does not rotate) has order one if and only if the line $\mathcal{C}$ is parallel to the projection plane Π. If $\mathcal{C}$ is parallel to the rolling-shutter lines on Π, then the RS_1 camera is of type II. Otherwise, it is of type I.*

The joint parameter space is

$$\begin{aligned}\mathcal{P}^{\mathrm{cs}}_{1}:=\{&(R,\mathcal{C},C) \mid R=\left[\begin{smallmatrix}w_1\\w_2\\w_3\end{smallmatrix}\right]\in\mathrm{SO}(3),\\ &\mathcal{C}\in\mathrm{Gr}(1,\mathbb{P}^3),\ \mathcal{C}\neq\mathcal{C}^\infty\in(w_1:0)\vee(w_2:0),\\ &C:\mathbb{P}^1\dashrightarrow\mathcal{C} \text{ birational},\ C(1:0)=\mathcal{C}^\infty\}.\end{aligned} \tag{18}$$

The parameters with $\mathcal{C}^\infty=(w_2:0)$ correspond to type-II cameras; the others to type-I cameras.

Remark 11. A linear RS camera whose center moves on a line that is *not* parallel to the projection plane has order two.

5. The image of a line

RS_1 cameras view 3D points exactly once. So their image of a 3D line is an irreducible curve. However, that curve is typically not a line. The degree of that image curve is the degree of the picture-taking map Φ in (7).

Theorem 12. *The degree of Φ for a general RS_1 camera in the parameter spaces described above is*

$\mathcal{P}_{I,d,\delta}$	$\mathcal{P}^{\mathrm{cs}}_{I,1,\delta}$	$\mathcal{P}_{II,d,\delta}$	$\mathcal{P}^{\mathrm{cs}}_{II,1,\delta}$	$\mathcal{P}_{I,d}$	$\mathcal{P}^{\mathrm{cs}}_{I,1}$	$\mathcal{P}_{II,d}$	$\mathcal{P}^{\mathrm{cs}}_{II,1}$
$2d+\delta+1$	$\delta+3$	$2d+\delta+2$	$\delta+4$	$d+1$	2	$d+1$	2

The image curve of a line under an RS_1 camera is not an arbitrary rational curve of the degree as prescribed in Theorem 12. In fact, they have a single singularity at the image point where all rolling lines meet.

Proposition 13. *Consider an RS_1 camera. For a general line L, its image $\Phi(L)$ is a curve of degree $\deg(\Phi)$ with multiplicity $\deg(\Phi)-1$ at the point $(0:1:0)$.*

6. Minimal problems of linear RS_1 cameras

The linear RS_1 cameras are classified in Proposition 10. This section classifies the minimal problems of structure-from-motion (SfM) from linear RS_1 cameras that observe points, lines, and their incidences. In this setting, SfM is the following 3D reconstruction problem:

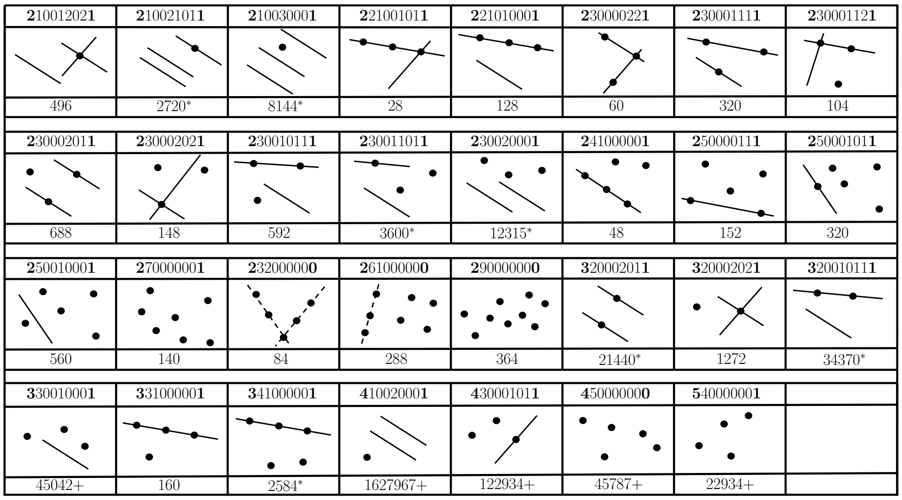

Figure 4. Illustration of all minimal problems as lines and points in $\mathbb{P}^3$. Each problem is encoded by 9 integers: The number m of cameras, followed by its combinatorial signature (see Definition 42 ff.) with p_∞ at the end. Points on dashed lines are known to be collinear in $\mathbb{P}^3$, but the image conics are not observed. Lower bounds for the degrees are shown below the sketches, see Remark 49. "$*$": the maximum from different computational runs is shown (the actual number is close to the number shown). "$+$": interrupted runs (the actual number is higher than the number shown).

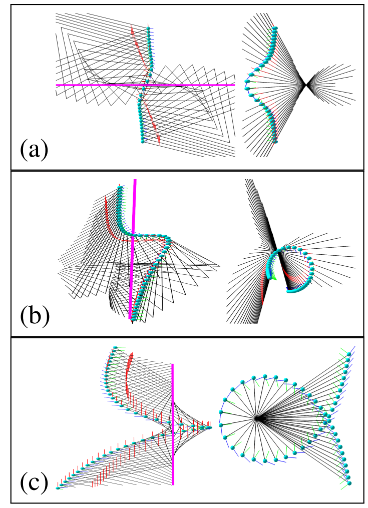

Figure 5. (a) Example 21, (b) Example 22, (c) Example 23. The camera center C (cyan) moves along a twisted cubic curve $\mathcal{C}$. The rolling planes Σ (black) intersect in a line K (magenta). See Sec. 11 for more details.

Problem 14. We have pictures $Y_1, \ldots, Y_m$ of a finite set X of points and lines in space. The points and lines in X satisfy some prescribed incidences. Each picture was taken by a linear RS_1 camera. Find the set X and the camera parameters that produced the pictures.

Let $\mathcal{P}^m$ be the set of all m-tuples of camera parameters. We can take $\mathcal{P}^m = (\mathcal{P}_1^{\text{cs}})^m$, where the latter parameter space is defined in (18). We consider point-line arrangements in 3-space consisting of p points and ℓ lines whose incidences are encoded by an index set $\mathcal{I} \subset [p] \times [\ell]$. That $(i, j) \in \mathcal{I}$ means that the i-th point is contained in the j-th line. We model intersecting lines by requiring their intersection point to be one of the p points. We write $\mathfrak{X} = \mathfrak{X}(p, \ell, \mathcal{I})$ for the variety of all p-tuples of points and ℓ-tuples of lines in space that satisfy the incidences prescribed by $\mathcal{I}$.

By Theorem 12, a general linear RS_1 camera maps a general line in space to an image conic. The next lemma explains that the line at infinity on the image plane intersects each image conic at two points: one is $(0:1:0)$, the other depends only on the camera parameters.

Lemma 15. *Let $(R, \mathcal{C}, C) \in \mathcal{P}_1^{cs}$ be of type I and $(a:b:0)$ be such that $\mathcal{C}^\infty = (a:b:0) \cdot R$. Consider the associated picture-taking map $\Phi\colon \mathbb{P}^3 \dashrightarrow \mathbb{P}^2$ and a line $L \subset \mathbb{P}^3$. Then:*
- *either $\overline{\Phi(L)}$ is a conic through $(0:1:0)$ and $(a:b:0)$,*
- *or $\overline{\Phi(L)}$ is the line through $(0:1:0)$ and $(a:b:0)$.*

Hence, the camera maps a general point-line arrangement in $\mathfrak{X}$ to an arrangement in the image plane consisting of p points and ℓ conics that satisfy the incidences $\mathcal{I}$ and such that all conics pass through the same two points at infinity, one of them being $(0:1:0)$. We write $\mathcal{Y}(p, \ell, \mathcal{I})$ for the variety of all such planar point-conic arrangements.

Note that, as soon as such an arrangement contains at least one conic, the point $(a:b:0)$ from Lemma 15 is known. It can be obtained from intersecting the conic with the line at infinity. If however only image points have been observed, then the point $(a:b:0)$ is a priori unknown. But we might have an oracle that has additional knowledge of camera parameters and provides us with that special point. Thus, we want to allow the possible knowledge of the point $(a:b:0)$ for each involved camera, without necessarily observing any image conics. We set the boolean value $p_\infty \in \{1, 0\}$ according to whether we assume knowledge of the point $(a:b:0)$ or not. We write $\mathcal{Y} = \mathcal{Y}(p, \ell, \mathcal{I}, p_\infty)$ for the variety of all planar point-conic arrangements in $\mathcal{Y}(p, \ell, \mathcal{I})$ plus the point $(a:b:0)$ if $p_\infty = 1$.

Problem 14 asks to compute the preimage of such a planar arrangement $y \in \mathcal{Y}$ under the rational joint-camera map $\mathcal{P}^m \times \mathfrak{X} \dashrightarrow \mathcal{Y}$. The scaled special Euclidean group G from Remark 1 acts on the preimages of that map, so we rather consider the quotient on the domain and let $\Phi^{(m)} = \Phi^{(m)}(p, \ell, \mathcal{I})$ be the map

$$\Phi^{(m)} : (\mathcal{P}^m \times \mathfrak{X})/G \dashrightarrow \mathcal{Y}. \tag{19}$$

Definition 16. The Reconstruction Problem 14 is *minimal* if its solution set is non-empty and finite for generic input pictures. In that case, the number of complex solutions given a generic input is the *degree* of the minimal problem.

Theorem 17. *There are exactly 31 minimal problems for SfM with linear RS_1 cameras fully observing point-line arrangements, where either all or no given views know the special point $(a\!:\!b\!:\!0)$. They are shown in Fig. 4.*

7. Straight-Cayley cameras

In [7], the Straight-Cayley RS model with a constant speed translation in the camera coordinate system β_u and Cayley rotation parameterization was used to set up a tractable minimal problem of RS absolute pose camera computation:

$$\begin{aligned}\lambda[u\,v\,1]^\top &= R\left((u-u_0)\,O_\delta\right)\,X_\delta + T_{\beta_u} + (u-u_0)\,V_{\beta_u}\\ R(c) &= \frac{1}{d}\begin{bmatrix}1+c_1^2-c_2^2-c_3^2 & 2\,(c_1c_2-c_3) & 2\,(c_1c_3+c_2)\\ 2\,(c_1c_2+c_3) & 1-c_1^2+c_2^2-c_3^2 & 2\,(c_2c_3-c_1)\\ 2\,(c_1c_3-c_2) & 2\,(c_2c_3+c_1) & 1-c_1^2-c_2^2+c_3^2\end{bmatrix} \qquad (20)\\ d &= 1+c_1^2+c_2^2+c_3^2\end{aligned}$$

Here, we have depth $\lambda \in \mathbb{R}$, image coordinates $u, v \in \mathbb{R}$, the offset $u_0 \in \mathbb{R}$, a rotation axis $O_\delta \in \mathbb{R}^3$ in the world coordinate system δ, a 3D point $X_\delta \in \mathbb{R}^3$, a camera center $T_{\beta_u} \in \mathbb{R}^3$ for $u = u_0$ in the cameras coordinate system β_u, and a translation direction vector $V_{\beta_u} \in \mathbb{R}^3$. The translation velocity is given by $\|V_\delta\| = \|V_{\beta_u}\|$. The rotation angle θ of $R\left((u-u_0)\,O_\delta\right)$ around the axis o is determined by $(u-u_0)\|O_\delta\| = \tan(\theta/2)$. Thus, for small angles, $\theta \simeq (u-u_0)\|O_\delta\|/2$, and $\|O_\delta\|/2$ approximates the angular velocity of the rotation. We now show how the camera center moves in the world coordinate system δ. We can write

$$\begin{aligned}\lambda[u\,v\,1]^\top = R((u-u_0)\,O_\delta)\,\cdot \qquad\qquad (21)\\ \Big(X_\delta - R((u-u_0)\,O_\delta)^\top\left(-T_{\beta_u} - (u-u_0)\,V_{\beta_u}\right)\Big),\end{aligned}$$

so the camera center in the world coordinate system δ is

$$C_\delta(u) = -R((u-u_0)O_\delta)^\top\left(T_{\beta_u} + (u-u_0)V_{\beta_u}\right). \quad (22)$$

Proposition 18. *For generic choices of the parameters $O_\delta, T_{\beta_u}, V_{\beta_u}$, the curve $\mathcal{C}$ parametrized by C_δ is a twisted cubic curve and the RS camera has order four.*

We are interested in understanding when such a camera has order one and falls into the setting of this paper. Recall that a necessary condition for order one is that all rolling planes intersect in a line.

Theorem 19. *All rolling planes intersect in a line if and only if the parameters $O_\delta = (o_1, o_2, o_3), T_{\beta_u} = (t_1, t_2, t_3), V_{\beta_u} = (v_1, v_2, v_3)$ satisfy one of the following:*
1. $v_3 = 0$, $o_3 = 0$, and $o_2 = -1$; or
2. $v_3 = 0$, $o_1 = 0$, and $o_2^2 + o_3^2 + o_2 = 0$; or
3. $v_3 = 0$, $v_1 = t_3$, $t_1 = 0$, $o_1 = 0$, and $o_3 = 0$.
In each case, the camera-center curve $\mathcal{C}$ is generically still a twisted cubic curve. In the first two cases, the RS camera has order one. In the third case, the RS camera has generically order three, and its order is one if and only if the parameters also satisfy the conditions in either 1. or 2.

Thus, the first 2 cases of Thm. 19 describe all RS_1 cameras.

Proposition 20. *For both cases of RS_1 cameras, the picture-taking map Φ is generically of degree four: it maps generic lines in space to quartic image curves.*

Example 21 ($O_\delta = (1,-1,0), T_{\beta_u} = (0,0,1), V_{\beta_u} = (0,1,0)$). This is an example of case 1 in Theorem 19. The camera center moves on the twisted cubic curve defined by $X_1X_3 - X_2X_3 + X_2X_0 = 2X_2^2 + X_3^2 + X_3X_0 = 2X_1X_2 + X_3^2 - X_0^2 = 0$. The line K, which is the intersection of all rolling planes, is defined by $X_1 = 0$ and $X_3 = X_0$. It intersects the twisted cubic $\mathcal{C}$ at two complex conjugated points. The picture-taking map $\Phi : \mathbb{P}^3 \dashrightarrow \mathbb{P}^2$ sends $(X_1 : X_2 : X_3 : X_0)$ to

$$\begin{pmatrix} -2X_1^2X_2X_3 - X_1X_3^3 + 2X_1^2X_2X_0 + X_1X_3^2X_0 + X_1X_3X_0^2 - X_1X_0^3\\ -2X_1^3X_3 - 2X_1X_3^3 + X_2X_3^3 + 3X_1X_3^2X_0 - 3X_2X_3^2X_0 + 3X_2X_3X_0^2 - X_1X_0^3 - X_2X_0^3\\ 2X_1X_2X_3^2 + X_3^4 - 4X_1X_2X_3X_0 - 2X_3^3X_0 + 2X_1X_2X_0^2 + 2X_3X_0^3 - X_0^4\end{pmatrix}.$$

Example 22 ($O_\delta = (0,-\frac{1}{2},\frac{1}{2}), T_{\beta_u} = (0,0,1), V_{\beta_u} = (0,1,0)$). This is an example of case 2 in Theorem 19. The camera center moves on the twisted cubic curve defined by $X_1X_2 - X_1X_3 - X_1X_0 + 2X_3X_0 + 2X_0^2 = X_1^2 + 2X_2X_3 + 2X_2X_0 - 2X_3X_0 - 2X_0^2 = X_2^2 - X_2X_3 - X_1X_0 - 2X_2X_0 + X_3X_0 + X_0^2 = 0$. The line K, the intersection of all rolling planes, is defined by $X_1 = 0$, $X_2 = X_0$. It meets the twisted cubic $\mathcal{C}$ at the points $(0:0:1:0)$ and $(0:1:-1:1)$. The picture-taking map $\Phi : \mathbb{P}^3 \dashrightarrow \mathbb{P}^2$ sends $(X_1 : X_2 : X_3 : 1)$ to

$$\begin{pmatrix} -X_1^3X_2 - 2X_1X_2^2X_3 + X_1^3 - 2X_1X_2^2 + 4X_1X_2X_3 + 4X_1X_2 - 2X_1X_3 - 2X_1\\ 2X_1^2X_2^2 + 2X_2^4 - X_1^2X_2X_3 - X_1^3 - 4X_1^2X_2 - 2X_1X_2^2 -\\ \qquad -6X_2^3 + X_1^2X_3 + 2X_1^2 + 4X_1X_2 + 6X_2^2 - 2X_1 - 2X_2\\ X_1^2X_2^2 + 2X_2^3X_3 - 2X_1^2X_2 + 2X_2^3 - 6X_2^2X_3 + X_1^2 - 6X_2^2 + 6X_2X_3 + 6X_2 - 2X_3 - 2\end{pmatrix}.$$

Example 23 ($O_\delta = (0,1,0), T_{\beta_u} = (0,0,1), V_{\beta_u} = (1,1,0)$). This is an example of case 3 in Theorem 19. The camera center moves on the twisted cubic curve defined by $X_2X_3 + X_1X_0 - 2X_2X_0 = X_1X_2 + X_2^2 - X_3X_0 - X_0^2 = X_1^2 - X_2^2 + X_3^2 - X_0^2 = 0$. The line K, which is the intersection of all rolling planes, is defined by $X_1 = 0$ and $X_3 = 0$. It does not meet the twisted cubic curve $\mathcal{C}$.

8. Conclusion

We provided a new model of RS cameras and characterized RS_1 cameras whose picture-taking process is encoded in a rational map. We described parameter spaces of RS_1 cameras and how images of lines taken by such cameras look. We classified all point-line minimal problems for linear RS_1 cameras and discovered new problems with few solutions and image features. In future work, we plan to implement and test the practicality of those new minimal solvers. For the found minimal problems with higher degrees, we plan to investigate whether they decompose into smaller problems via monodromy groups [13]. We further plan to classify the minimal relative pose problems for the Straight-Cayley RS model to exhibit whether this model is not only practical for absolute, but also relative pose. Finally, we will analyze higher-order cameras and the affect of the order on relative pose problems.

References

[1] O. Ait-Aider and F. Berry. Structure and kinematics triangulation with a rolling shutter stereo rig. In *ICCV*, 2009. 1

[2] Omar Ait-aider, Nicolas Andreff, Jean Marc Lavest, and Philippe Martinet. Simultaneous object pose and velocity computation using a single view from a rolling shutter camera. In *ECCV*, pages 56–68, 2006. 1

[3] Cenek Albl, Zuzana Kukelova, and Tomas Pajdla. R6P – rolling shutter absolute pose problem. In *Proceedings of the IEEE Conference on Computer Vision and Pattern Recognition*, pages 2292–2300, 2015. 2

[4] Cenek Albl, Zuzana Kukelova, and Tomas Pajdla. R6P - rolling shutter absolute pose problem. In *CVPR*, 2015. 1

[5] Cenek Albl, Zuzana Kukelova, and Tomas Pajdla. Rolling shutter absolute pose problem with known vertical direction. In *CVPR*, 2016.

[6] Cenek Albl, Akihiro Sugimoto, and Tomas Pajdla. Degeneracies in rolling shutter sfm. In *ECCV*, 2016.

[7] Cenek Albl, Zuzana Kukelova, Viktor Larsson, and Tomas Pajdla. Rolling shutter camera absolute pose. *IEEE Trans. Pattern Anal. Mach. Intell.*, 42(6):1439–1452, 2019. 2, 8

[8] Cenek Albl, Zuzana Kukelova, Viktor Larsson, Michal Polic, Tomas Pajdla, and Konrad Schindler. From two rolling shutters to one global shutter. In *Proceedings of the IEEE/CVF Conference on Computer Vision and Pattern Recognition*, pages 2505–2513, 2020.

[9] Fang Bai, Agniva Sengupta, and Adrien Bartoli. Scanline homographies for rolling-shutter plane absolute pose. In *IEEE/CVF Conference on Computer Vision and Pattern Recognition, CVPR 2022, New Orleans, LA, USA, June 18-24, 2022*, pages 8983–8992. IEEE, 2022.

[10] Guillaume Batog, Xavier Goaoc, and Jean Ponce. Admissible linear map models of linear cameras. In *The Twenty-Third IEEE Conference on Computer Vision and Pattern Recognition, CVPR 2010, San Francisco, CA, USA, 13-18 June 2010*, pages 1578–1585. IEEE Computer Society, 2010. 1

[11] Paul Breiding and Sascha Timme. HomotopyContinuation.jl: A package for homotopy continuation in julia, 2018. 2, 13

[12] Yuchao Dai, Hongdong Li, and Laurent Kneip. Rolling shutter camera relative pose: Generalized epipolar geometry. In *Proceedings of the IEEE Conference on Computer Vision and Pattern Recognition*, pages 4132–4140, 2016. 1, 2, 6

[13] Timothy Duff, Viktor Korotynskiy, Tomas Pajdla, and Margaret H Regan. Galois/monodromy groups for decomposing minimal problems in 3d reconstruction. *SIAM Journal on Applied Algebra and Geometry*, 6(4):740–772, 2022. 8

[14] Ph Ellia and Davide Franco. Gonality, clifford index and multisecants. *Journal of Pure and Applied Algebra*, 158(1): 25–39, 2001. 5

[15] Ricardo Fabbri, Timothy Duff, Hongyi Fan, Margaret H. Regan, David da Costa de Pinho, Elias P. Tsigaridas, Charles W. Wampler, Jonathan D. Hauenstein, Peter J. Giblin, Benjamin B. Kimia, Anton Leykin, and Tomas Pajdla. Trifocal relative pose from lines at points. *IEEE Trans. Pattern Anal. Mach. Intell.*, 45(6):7870–7884, 2023. 2

[16] Bin Fan and Yuchao Dai. Inverting a rolling shutter camera: Bring rolling shutter images to high framerate global shutter video. In *2021 IEEE/CVF International Conference on Computer Vision, ICCV 2021, Montreal, QC, Canada, October 10-17, 2021*, pages 4208–4217. IEEE, 2021. 1

[17] Bin Fan, Yuchao Dai, Zhiyuan Zhang, and Ke Wang. Differential sfm and image correction for a rolling shutter stereo rig. *Image Vis. Comput.*, 124:104492, 2022.

[18] Bin Fan, Yuchao Dai, and Mingyi He. Rolling shutter camera: Modeling, optimization and learning. *Mach. Intell. Res.*, 20(6):783–798, 2023.

[19] Bin Fan, Yuchao Dai, and Hongdong Li. Rolling shutter inversion: Bring rolling shutter images to high framerate global shutter video. *IEEE Trans. Pattern Anal. Mach. Intell.*, 45(5):6214–6230, 2023. 1

[20] Daniel R. Grayson and Michael E. Stillman. Macaulay2, a software system for research in algebraic geometry. `http://www2.macaulay2.com`. 12, 15

[21] Richard Hartley and Andrew Zisserman. *Multiple View Geometry in Computer Vision*. Cambridge, 2nd edition, 2003. 3

[22] Richard Hartley and Andrew Zisserman. *Multiple view geometry in computer vision*. Cambridge university press, 2003. 2

[23] Richard I. Hartley and Rajiv Gupta. Linear pushbroom cameras. In *Computer Vision - ECCV'94, Third European Conference on Computer Vision, Stockholm, Sweden, May 2-6, 1994, Proceedings, Volume I*, pages 555–566. Springer, 1994. 2

[24] Johan Hedborg, Per-Erik Forssén, Michael Felsberg, and Erik Ringaby. Rolling shutter bundle adjustment. In *CVPR*, 2012. 1

[25] Petr Hruby, Timothy Duff, Anton Leykin, and Tomas Pajdla. Learning to solve hard minimal problems. In *IEEE/CVF Conference on Computer Vision and Pattern Recognition, CVPR 2022, New Orleans, LA, USA, June 18-24, 2022*, pages 5522–5532. IEEE, 2022. 2

[26] Petr Hruby, Viktor Korotynskiy, Timothy Duff, Luke Oeding, Marc Pollefeys, Tomas Pajdla, and Viktor Larsson. Four-view geometry with unknown radial distortion. In *IEEE/CVF Conference on Computer Vision and Pattern Recognition, CVPR 2023, Vancouver, BC, Canada, June 17-24, 2023*, pages 8990–9000. IEEE, 2023. 2

[27] Eisuke Ito and Takayuki Okatani. Self-Calibration-Based Approach to Critical Motion Sequences of Rolling-Shutter Structure From Motion. In *CVPR*, 2017. 1

[28] Charles Minshall Jessop. *A Treatise on the Line Complex*. Cambridge University Press, 1903. 4

[29] Praveen K, Lokesh Kumar T, and A. N. Rajagopalan. Deep network for rolling shutter rectification. *CoRR*, abs/2112.06170, 2021. 1

[30] Z. Kukelova, M. Bujnak, and T. Pajdla. Automatic Generator of Minimal Problem Solvers. In *ECCV*, 2008. 2

[31] Zuzana Kukelova, Cenek Albl, Akihiro Sugimoto, and Tomas Pajdla. Linear solution to the minimal absolute pose rolling shutter problem. In *ACCV*, 2018. 1

[32] Ernst Eduard Kummer. *Über die algebraischen Strahlensysteme, in's Besondere über die der ersten und zweiten Ordnung*. Königl. Akademie der Wissenschaften zu Berlin, 1866. 2

[33] Yizhen Lao and Omar Ait-Aider. A robust method for strong rolling shutter effects correction using lines with automatic feature selection. In *CVPR*, 2018. 1

[34] Yizhen Lao, Omar Ait-Aider, and Adrien Bartoli. Solving rolling shutter 3d vision problems using analogies with non-rigidity. *Int. J. Comput. Vis.*, 129(1):100–122, 2021. 1

[35] Viktor Larsson, Magnus Oskarsson, Kalle Åström, Alge Wallis, Zuzana Kukelova, and Tomás Pajdla. Beyond grobner bases: Basis selection for minimal solvers. In *2018 IEEE Conference on Computer Vision and Pattern Recognition, CVPR 2018, Salt Lake City, UT, USA, June 18-22, 2018*, pages 3945–3954. Computer Vision Foundation / IEEE Computer Society, 2018. 2

[36] Patrick Le Barz. Formules pour les espaces multisécants aux courbes algébriques. *Comptes Rendus Mathematique*, 340 (10):743–746, 2005. 4

[37] Bangyan Liao, Delin Qu, Yifei Xue, Huiqing Zhang, and Yizhen Lao. Revisiting rolling shutter bundle adjustment: Toward accurate and fast solution. In *IEEE/CVF Conference on Computer Vision and Pattern Recognition, CVPR 2023, Vancouver, BC, Canada, June 17-24, 2023*, pages 4863–4871. IEEE, 2023. 1

[38] Ludovic Magerand, Adrien Bartoli, Omar Ait-Aider, and Daniel Pizarro. Global optimization of object pose and motion from a single rolling shutter image with automatic 2d-3d matching. In *ECCV*, 2012. 1

[39] Evgeniy Martyushev, Jana Vráblíková, and Tomas Pajdla. Optimizing elimination templates by greedy parameter search. In *Proceedings of the IEEE/CVF Conference on Computer Vision and Pattern Recognition (CVPR)*, pages 15754–15764, 2022. 2

[40] Hermes McGriff, Renato Martins, Nicolas Andreff, and Cédric Demonceaux. Joint 3d shape and motion estimation from rolling shutter light-field images. In *IEEE/CVF Winter Conference on Applications of Computer Vision, WACV 2024, Waikoloa, HI, USA, January 3-8, 2024*, pages 3687–3696. IEEE, 2024. 1

[41] Marci Meingast, Christopher Geyer, and Shankar Sastry. Geometric models of rolling-shutter cameras. In *Omnidirectional Vision, Camera Networks and Non-classical Cameras*, 2005. 1

[42] Muyao Niu, Tong Chen, Yifan Zhan, Zhuoxiao Li, Xiang Ji, and Yinqiang Zheng. Rs-nerf: Neural radiance fields from rolling shutter images. In *Computer Vision - ECCV 2024 - 18th European Conference, Milan, Italy, September 29-October 4, 2024, Proceedings, Part XLVI*, pages 163–180. Springer, 2024. 1

[43] Luc Oth, Paul Timothy Furgale, Laurent Kneip, and Roland Siegwart. Rolling Shutter Camera Calibration. In *CVPR*, 2013. 1

[44] Tomas Pajdla. Stereo with oblique cameras. *Int. J. Comput. Vis.*, 47(1-3):161–170, 2002. 3

[45] Pietro De Poi. Congruences of lines with one-dimensional focal locus. *Portugaliae Mathematica*, 61:329–338, 2004. 2

[46] Jean Ponce. What is a camera? In *2009 IEEE Computer Society Conference on Computer Vision and Pattern Recognition (CVPR 2009), 20-25 June 2009, Miami, Florida, USA*, pages 1526–1533. IEEE Computer Society, 2009. 3

[47] Jean Ponce, Bernd Sturmfels, and Mathew Trager. Congruences and concurrent lines in multi-view geometry. *Advances in Applied Mathematics*, 88:62–91, 2017. 3

[48] Jean Ponce, Bernd Sturmfels, and Mathew Trager. Congruences and concurrent lines in multi-view geometry. *Advances in Applied Mathematics*, 88:62–91, 2017. 4, 5

[49] Pulak Purkait and Christopher Zach. Minimal solvers for monocular rolling shutter compensation under ackermann motion. In *WACV*, 2018. 1

[50] Olivier Saurer, Kevin Köser, Jean-Yves Bouguet, and Marc Pollefeys. Rolling Shutter Stereo. In *ICCV*, 2013.

[51] Olivier Saurer, Marc Pollefeys, and Gim Hee Lee. A minimal solution to the rolling shutter pose estimation problem. In *IROS*, 2015. 1

[52] Steven M. Seitz and Jiwon Kim. The space of all stereo images. *Int. J. Comput. Vis.*, 48(1):21–38, 2002. 3

[53] Matthew Trager, Bernd Sturmfels, John F. Canny, Martial Hebert, and Jean Ponce. General models for rational cameras and the case of two-slit projections. *CoRR*, abs/1612.01160, 2016. 3

[54] Subeesh Vasu, Mahesh Mohan M. R., and A. N. Rajagopalan. Occlusion-Aware Rolling Shutter Rectification of 3d Scenes. In *CVPR*, 2018. 1

[55] Yongcong Zhang, Bangyan Liao, Yifei Xue, Chen Lu, Peidong Liu, and Yizhen Lao. RSL-BA: rolling shutter line bundle adjustment. *CoRR*, abs/2408.05409, 2024.

[56] Zhihang Zhong, Yinqiang Zheng, and Imari Sato. Towards rolling shutter correction and deblurring in dynamic scenes. In *IEEE Conference on Computer Vision and Pattern Recognition, CVPR 2021, virtual, June 19-25, 2021*, pages 9219–9228. Computer Vision Foundation / IEEE, 2021.

[57] Bingbing Zhuang, Loong-Fah Cheong, and Gim Hee Lee. Rolling-Shutter-Aware Differential SfM and Image Rectification. In *ICCV*, 2017.

[58] Bingbing Zhuang, Quoc-Huy Tran, Pan Ji, Loong-Fah Cheong, and Manmohan Chandraker. Learning structure-and-motion-aware rolling shutter correction. In *CVPR*, 2019. 1